

Superfluid weight and Berezinskii-Kosterlitz-Thouless transition temperature of strained graphene

Feng Xu,^{1,2,*} Lei Zhang,^{1,2} Liyun Jiang,^{1,2} and Chung-Yu Mou^{3,4,†}

¹*School of Physics and Telecommunication Engineering,
Shaanxi University of technology, Hanzhong 723001, China*

²*Institute of Graphene at Shaanxi Key Laboratory of Catalysis,
Shaanxi University of technology, Hanzhong 723001, China*

³*Physics Division, National Center for Theoretical Sciences,
P.O.Box 2-131, Hsinchu, Taiwan, R.O.C.*

⁴*Center for Quantum Technology and Department of Physics,
National Tsing Hua University, Hsinchu 30043, Taiwan, R.O.C.*

Abstract

We obtain the superfluid weight and Berezinskii-Kosterlitz-Thouless (BKT) transition temperature for highly unconventional superconducting states with the coexistence of chiral d-wave superconductivity, charge density waves and pair density waves in the strained graphene. Our results show that the strain-induced flat bands can promote the superconducting transition temperature approximately 50% compared to that of the original doped graphene, which suggests that the flat-band superconductivity is a potential route to get superconductivity with higher critical temperatures. In particular, we obtain the superfluid weight for the pure superconducting pair-density-wave states from which the deduced superconducting transition temperature is shown to be much lower than the gap-opening temperature of the pair density wave, which is helpful to understand the phenomenon of the pseudogap state in high- T_c cuprate superconductors. Finally, we show that the BKT transition temperature versus doping for strained graphene exhibits a dome-like shape and it depends linearly on the spin-spin interaction strength.

I. INTRODUCTION

Graphene is one of the most exciting novel materials and has become a goldmine for fascinating physics^{1,2}. A large number of exotic superconducting states of graphene, such as the extend s -wave superconducting state, the chiral d -wave superconducting state, $p + ip$ -wave superconducting state, have been proposed theoretically after considering the interaction and correlation effects between electrons³⁻⁸. The chiral superconductivity breaks both time-reversal and parity symmetries, which is a natural extension of the d -wave state on the square lattice to honeycomb lattice due to the sixfold symmetry. The graphene, when it is doped to the level ($\frac{1}{4}$ hole-doping) with the van Hove singularity, is particularly proposed to be a chiral d -wave superconductor⁹.

The recent realization of superconducting state in a twisted bilayer graphene has inspired reconsideration of theories about the superconductivity that occurs in dispersionless bands¹⁰⁻¹². It is well known that in 3D, the superconducting critical temperature T_c in the BCS theory depends exponentially on product of the electronic density of states and the strength of attractive interaction in conventional superconductors. It is then a natural proposal to increase the density of states in the searching of superconductors with higher critical temperatures¹³. An extreme route to increase the density of states is proposed by considering pairing in the flat band, which has been shown that in 3D, the superconducting transition temperature in the BCS theory linearly depends on the electron-phonon coupling constant¹⁴⁻¹⁷. However, since the electronic states in the flat band tend to be more localized, the electron-electron interaction is much stronger in flat-bands. It is therefore necessary to examine how the superconducting transition temperature behaves in flat-bands with strong correlation.

An easy route to realize flat bands in graphene is proposed recently by considering the periodic strain¹⁸. By considering the strong electron-electron interaction limit, even more exciting, it shows that the long-sought-after superconducting states with non-vanishing center-of-mass momentum for Cooper pairs (the superconducting pair-density-wave states) can be also realized¹⁹⁻²². Nonetheless, since graphene is a two-dimensional matter, instead of being determined by vanishing of the superconducting order parameter, the superconducting transition is determined by the Berezinskii-Kosterlitz-Thouless (BKT) temperature T_{BKT} , which is defined as $k_B T_{BKT} = \frac{\pi \hbar^2 n_s}{8m}$, where n_s is the superfluid

weight²³⁻³⁰. It is therefore crucial to examine the BKT transition in strained graphene with strong correlation.

In this paper, we investigate the superfluid weight and Berezinskii-Kosterlitz-Thouless (BKT) transition temperature for highly unconventional superconducting states that occur in flat-band of the strained graphene with strong correlation. We will first compute the superfluid weight and BKT transition temperature for the chiral d-wave superconducting state that coexists with the charge density wave and the pair density wave. We will show that the strain-induced flat bands enhance the superconducting critical temperature (defined as the BTK transition temperature) approximately 50% in comparison to that of unstrained graphene. Secondly, we compute the superfluid weight of a pure superconducting pair-density-wave state that emerges in the lightly doped graphene and find that the BKT transition temperature is much lower than the temperature when the order of the pair density wave vanishes. This phenomenon is similar to the pseudogap state observed in the cuprate superconductor. Finally, we show that the dependence of the critical temperature on doping exhibits a dome-like shape in resemblance to the superconducting dome observed in high- T_c cuprate superconductors¹³ and twisted bilayer graphene¹². Furthermore, in the strong correlation limit, the critical temperature depends the residual spin-spin interaction strength linearly. The effect of amplitude and period of strain on the superfluid weight will be discussed at the end. This paper is organized as follows. In Sec. II, we describe the basic theoretical model and formulation for computing the superfluid weight and the Berezinskii-Kosterlitz-Thouless (BKT) transition temperature for strained graphene. In Sec. III, we present our numerical results and discuss their physical meanings. Finally, conclusions are drawn in Sec. IV.

II. THEORETICAL FORMULATION

The graphene with periodic strain can be achieved in experiments through the presence of ripples with fixed period L or by external stretching as shown in the Fig. 1(b). Theoretically, the strain generally induces changes of hopping amplitudes for electrons. In the tight-binding limit, we shall keep hopping amplitudes to the nearest-neighbors that are characterized by three vectors \vec{e}_1 , \vec{e}_2 , and \vec{e}_3 as shown in Fig. 1(a), where $\vec{e}_1 = \frac{a}{2}(1, \sqrt{3})$, $\vec{e}_2 = \frac{a}{2}(1, -\sqrt{3})$, and $\vec{e}_3 = -a(1, 0)$. The equilibrium hopping amplitude $t = 2.8eV$

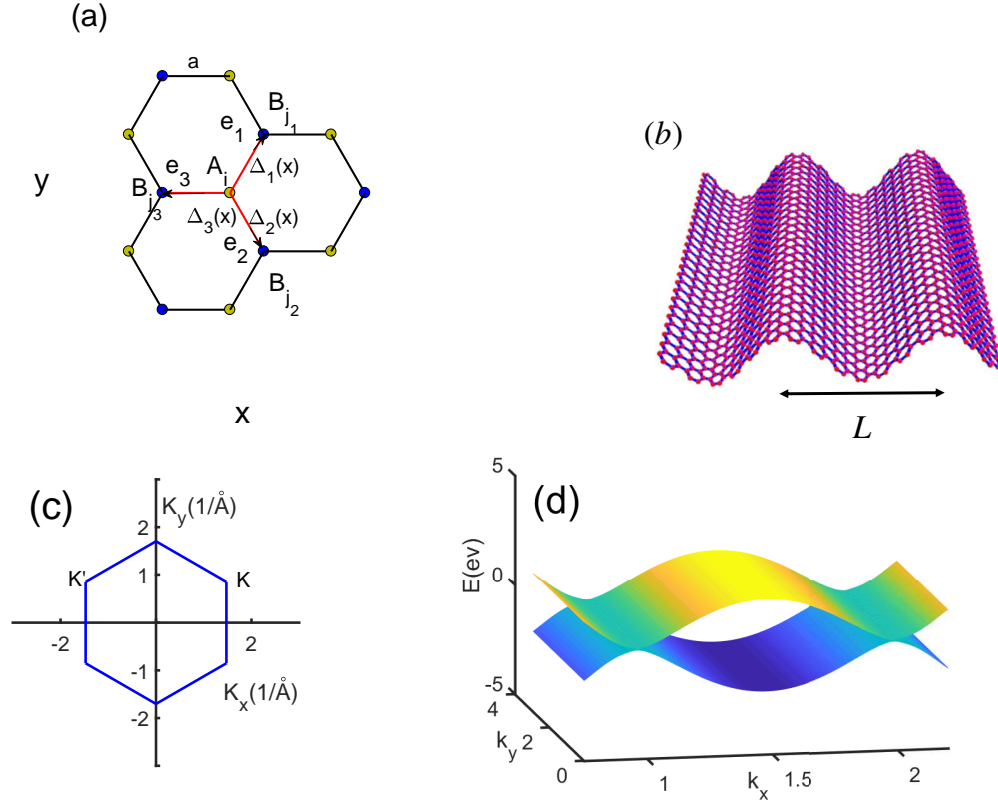


FIG. 1. Topological flat bands in periodically strained graphene: (a) Honeycomb lattice of graphene, where $e_{i=1,2,3}$ are the nearest-neighbor vectors and $\Delta_{i=1,2,3}(x)$ represents three superconducting orders. (b) Schematic plot of strained graphene. (c) First Brillouin zone of graphene. (d) Lowest energy spectrum of graphene that exhibits flat-bands.

is fixed and $a = 1.42\text{\AA}$ is the equilibrium bond length. The deformed bond for the strain will be assumed to be the nearest-neighbor bond associated with $e_3 = -a(1,0)$ and the periodically-modified hopping amplitudes are consistent with the strain period $L = \frac{3na}{2}$, where $n = 2, 3, 4, \dots$. The tight-binding Hamiltonian of periodically strained graphene is thus given by

$$\mathcal{H}_0 = - \sum_{i,j_1,\sigma} t a_{i,\sigma}^\dagger b_{j_1,\sigma} - \sum_{i,j_2,\sigma} t a_{i,\sigma}^\dagger b_{j_2,\sigma} - \sum_{i,j_3,\sigma} (t + \delta t \cos \frac{2\pi x_i}{L}) a_{i,\sigma}^\dagger b_{j_3,\sigma} + h.c., \quad (1)$$

where $a_{i,\sigma}$ ($a_{i,\sigma}^\dagger$) annihilates (creates) an electron with spin σ on site R_i of sublattice A (an equivalent definition for $b_{i,\sigma}$ and $b_{i,\sigma}^\dagger$ is used for sublattice B) and $R_{j_k} = R_i + e_k$. The first Brillouin zone of graphene without strain is plotted in the Fig.1(c). In the presence of strain, the lowest energy spectrum of graphene in the normal state is shown in the

Fig. 1(d). Clearly, it exhibits flat bands in the k_y direction. The strong correlation is included by considering the Hubbard interaction between electrons, $\mathbf{U} \sum_i n_{i\uparrow} n_{i\downarrow}$. In the strong interacting limit, the singly occupied state can be described by an effective t-J model as follows^{31,32}

$$\mathcal{H} = P_G \left[\mathcal{H}_0 + \sum_{i,j} J_{ij} \left(\vec{S}_i \cdot \vec{S}_j - \frac{1}{4} n_i n_j \right) \right] P_G, \quad (2)$$

where $J_{ij} = \frac{4t_{ij}^2}{\mathbf{U}}$ is the antiferromagnetic (AF) coupling, \vec{S}_i and n_i are the spin and number operators for electrons at i site respectively, and $P_G = \prod_i (1 - n_{i\uparrow} n_{i\downarrow})$ is the Gutzwiller projection operator that projects out states with doubly-occupied sites. Note that J_{ij} acquires the spatial dependence through the deformed hopping amplitude. The parameters we shall use in this paper are as follows: $\mathbf{U} = 4t$, $J = \frac{4t^2}{\mathbf{U}}$, $t = 2.8$ eV, the period of strain $n = 15$, and the strain strength $\delta t/t = 0 \rightarrow 0.25$.

To investigate superconductivity of this model, the AF interaction term, $\vec{S}_i \vec{S}_j - \frac{1}{4} n_i n_j$, is decoupled into³³, $-\frac{3}{8} (\hat{\chi}_{ij}^\dagger \hat{\chi}_{ij} + \hat{\Delta}_{ij}^\dagger \hat{\Delta}_{ij})$, where $\hat{\chi}_{ij}^\dagger = \hat{c}_{i\uparrow}^\dagger \hat{c}_{j\uparrow} + \hat{c}_{i\downarrow}^\dagger \hat{c}_{j\downarrow}$ and $\hat{\Delta}_{ij}^\dagger = \hat{c}_{i\uparrow}^\dagger \hat{c}_{j\downarrow}^\dagger - \hat{c}_{i\downarrow}^\dagger \hat{c}_{j\uparrow}^\dagger$. We resort to the slave-boson method to investigate this strained graphene model in the mean-field level³³⁻³⁵. Since the slaved boson condenses in the superconducting state, the electron operator can be written as $c_{i\sigma} = \sqrt{\delta_i} f_{i\sigma}$, where δ_i is the hole density on site i and $f_{i\sigma}$ is the fermionic spinon operator. The mean-field Hamiltonian is then given by

$$\mathcal{H}_{MF} = \sum_{\langle ij \rangle, \sigma} -(\sqrt{\delta_i \delta_j} t_{ij} + \frac{3}{8} J_{ij} \chi_{ij}) \hat{f}_{i\sigma}^\dagger \hat{f}_{j\sigma} - \sum_{\langle ij \rangle} \frac{3}{8} J_{ij} \Delta_{ij} (\hat{f}_{i\uparrow}^\dagger \hat{f}_{j\downarrow}^\dagger - \hat{f}_{i\downarrow}^\dagger \hat{f}_{j\uparrow}^\dagger) + h.c. \quad (3)$$

Here $\chi_{ij} = \langle \hat{\chi}_{ij} \rangle$, $\Delta_{ij} = \langle \hat{\Delta}_{ij} \rangle$, and the doping level δ is the average of δ_i . To match with the periodic strain, it is presumed that χ_{ij} and Δ_{ij} depend on position as shown in the Fig. 1(b). The order parameters set as

$$\begin{aligned} \Delta_{ij} &= \Delta_0 + \langle \hat{\Delta}_{\frac{Q}{2}} \rangle \exp(i\frac{Q}{2}x) + \langle \hat{\Delta}_{-\frac{Q}{2}} \rangle \exp(-i\frac{Q}{2}x) + \langle \hat{\Delta}_Q \rangle \exp(iQx) + \langle \hat{\Delta}_{-Q} \rangle \exp(-iQx), \\ \chi_{ij} &= \chi_0 + \langle \hat{\chi}_Q \rangle \exp(iQx) + \langle \hat{\chi}_{-Q} \rangle \exp(-iQx), \end{aligned} \quad (4)$$

where $Q = \frac{2\pi}{L}$ corresponds to the period of strained graphene in the momentum space. In particular, Δ_{ij} has a period with $2L$ and when its spatial average vanishes, it corresponds to the form of the superconducting order parameter in the pure pair-density-wave state¹⁸. In the pure pair-density-wave state, we have $\Delta_0 = \langle \hat{\Delta}_Q \rangle = \langle \hat{\Delta}_{-Q} \rangle = 0$ and $\langle \hat{\Delta}_{\frac{Q}{2}} \rangle =$

$\langle \hat{\Delta}_{-\frac{Q}{2}} \rangle \neq 0$, which is similar to the Larkin-Ovchinnikov state with two complex order-parameters $\langle \hat{\Delta}_{\pm\frac{Q}{2}} \rangle$ and is different from the Fulde-Ferrell state in which there is only one complex order-parameter field $\langle \hat{\Delta}_{\frac{Q}{2}} \rangle$ ³⁹⁻⁴¹.

We perform a discrete Fourier transformation to the mean-field Hamiltonian with

$$\hat{C}_{i\sigma} = \frac{1}{N} \sum_{\mathbf{k}} \hat{C}_{\mathbf{k}\sigma} \exp i\mathbf{k}r, \quad (5)$$

the mean-field Hamiltonian can be then expressed as

$$H_{MF} = \sum_{\mathbf{k}, \sigma} \psi^\dagger(\mathbf{k}) h_{MF}(\mathbf{k}) \psi(\mathbf{k}), \quad (6)$$

where $\psi(\mathbf{k}) = (C_{A\uparrow, k_x + \frac{\pi j}{L}, k_y}^\dagger, C_{B\uparrow, k_x + \frac{\pi j}{L}, k_y}^\dagger, C_{A\downarrow, -k_x + \frac{\pi j}{L}, -k_y}, C_{B\downarrow, -k_x + \frac{\pi j}{L}, -k_y})$, $j = 0, 1, \dots, 2n - 1$. The Hamiltonian are then self-consistently solved with the chiral d-wave superconducting order Δ , $\exp(i\frac{2\pi}{3})\Delta$, $\exp(i\frac{4\pi}{3})\Delta$, hopping amplitude χ , charge density waves in hopping amplitude $\langle \hat{\chi}_Q \rangle$, pair density waves $\langle \hat{\Delta}_{\frac{Q}{2}} \rangle$, and $\langle \hat{\Delta}_Q \rangle$. The temperature-dependence of a mean-field order \hat{O} is obtained by the follow equation:

$$O(T) = \frac{1}{N} \sum_k \langle \hat{O} \rangle = \frac{1}{N} \sum_{nk} \langle \psi_{nk} | \hat{O} | \psi_{nk} \rangle \frac{1}{1 + \exp(\frac{E_{nk}}{k_B T})}, \quad (7)$$

where ψ_{nk} and E_{nk} are the eigenfunction and eigenvalue of the mean-field Hamiltonian and k_B is the Boltzmann constant and T is temperature. A flat energy band allows deformations of the particle momentum distribution without energy cost. The pair density wave state has been proposed as an alternative state that gives a lower energy than that of the conventional BCS state⁴¹. The phases diagram about those coexisting states in the ground state and its thermal effect has been discussed with the Ginzburg-Landau theory in the previous works^{18,22}. Here we focus on the superfluid weight and the Berezinskii-Kosterlitz-Thouless (BKT) transition temperature on this system and the optimal parameters to enhance the superconducting transition temperature.

To determine the superfluid weight, we resort to the linear response theory and compute the current-current correlation function³⁶⁻³⁸. The paramagnetic current density (x component) at the position r is defined as^{36,37}

$$J_x^P(r) = it \sum_{\sigma} (\hat{C}_{r+x\sigma}^\dagger \hat{C}_{r\sigma} - \hat{C}_{r\sigma}^\dagger \hat{C}_{r+x\sigma}), \quad (8)$$

and the kinetic energy density associated with x -oriented link at position r is given by

$$\hat{K}(r) = -t \sum_{\sigma} (\hat{C}_{r+x\sigma}^\dagger \hat{C}_{r\sigma} + \hat{C}_{r\sigma}^\dagger \hat{C}_{r+x\sigma}). \quad (9)$$

The kinetic energy density is numerically computed as follow:

$$\langle -K_x(T) \rangle = \delta \frac{t}{N} \sum_{nk\sigma} \langle \psi_{nk} | (C_{Bk\sigma}^\dagger C_{Ak\sigma} + C_{Ak\sigma}^\dagger C_{Bk\sigma}) | \psi_{nk} \rangle \frac{1}{1 + \exp\left(\frac{E_{nk}}{k_B T}\right)}, \quad (10)$$

where δ is the averaged hole doping level. The linear current response produced by the vector potential $A_x(r, t) = A_x(q) \exp(iqr - i\omega t)$ is given by

$$\langle J_x(q, \omega) \rangle = -e^2 [\langle -K_x \rangle - \Lambda_{xx}(q, \omega)] A_x(q, \omega), \quad (11)$$

where $J_x(q, \omega)$ is the total current and Λ_{xx} is the current-current correlation function for the paramagnetic current density^{36–38}, which is given by

$$\begin{aligned} J_x^P(k, q) &= it \sum_r e^{-iqr} (C_{j_3}^\dagger C_i - C_i^\dagger C_{j_3}) \\ &= it \sum_k \{ C_{Bk\sigma}^\dagger C_{A_{k+q\sigma}} - C_{A_{k\sigma}}^\dagger C_{B_{k+q\sigma}} \}. \end{aligned} \quad (12)$$

The current-current correlation function is then given by

$$\begin{aligned} \Lambda_{xx}(q, i\omega_m) &= \delta \frac{1}{N} \int_0^\beta e^{i\omega_m \tau} \langle J_x^P(q, \tau) J_x^P(-q, 0) \rangle \\ &= \delta \frac{1}{N} \sum_k J_x(k, q) J_x(-k, -q) \text{Tr} G_0(k+q, i\omega_m + i\Omega) G_0(k, i\Omega) (-1) \\ &= \delta \frac{t^2}{N} \sum_{k,n,m} \mathbf{U}^\dagger(k) \Xi \mathbf{U}(k+q) \mathbf{U}^\dagger(k+q) \Xi \mathbf{U}(k) \frac{f(E_n(k+q)) - f(E_m(k))}{E_n(k+q) - E_m(k) + i\omega_m}, \end{aligned} \quad (13)$$

where $\mathbf{U}(k) = (\psi_{1k}, \psi_{2k}, \dots, \psi_{nk})$, Ξ is the matrix form of J_x , $f(E_n)$ is the Fermi-Dirac distribution function, and $\omega_m = 2\pi m k_B T$ is the Matsubara frequency which will be set to $i\omega_m \rightarrow \omega + i\delta$ in the usual analytic continuation. Note that the current-current correlation function is related to the electric conductivity through the relation

$$\sigma_{xx}(\omega) = -e^2 \frac{\langle -K_x \rangle - \Lambda_{xx}(q=0, \omega)}{i(\omega + i\delta)}. \quad (14)$$

The superfluid weight D_s is then obtained by setting

$$\frac{D_s(T)}{\pi e^2} = \langle -K_x \rangle - \Lambda_{xx}(q_x = 0, q_y \rightarrow 0, i\omega_m = 0) \equiv \frac{n_s(T)}{m} \quad (15)$$

with the restricted condition $\langle -K(x) \rangle - \Lambda_{xx}(q_x \rightarrow 0, q_y = 0, i\omega_m = 0)$ as required by gauge invariance. This superfluid weight definition is equivalent to the one defined via the change of free energy due to the phase twist applied to the superconducting order parameter^{16,43}. Here the superfluid density $n_s(T)$ is determined through the superfluid

weight as $n_s(T) = m \frac{D_s}{\pi e^2}$ with m being the effective mass for the Cooper pair. By ignoring the anisotropic effect on the superfluid weight and assuming $D_s(x) = D_s(y)$ for simple computation, in fact, the superfluid weight on the y direction can be obtained in the same way.

As the strained graphene is a two-dimensional system, the critical temperature transition to superconductivity is determined by the Berezinskii-Kosterlitz-Thouless (BKT) transition temperature as^{23–25,42}

$$k_B T_{BKT} = \frac{\pi \hbar^2}{8} \frac{n_s(T_{BKT})}{m}. \quad (16)$$

Since the superfluid density $n_s(T)$ is obtained by numerical calculating Eq.10 and Eq.13, it is equivalent to the definition in terms of the stiffness of the superconducting order parameter in the thermodynamic potentials. The definition of the Berezinskii-Kosterlitz-Thouless (BKT) transition temperature has long applied in the multiband system with great success, such as twisted bilayer graphene with valence electrons and flat bands^{30,43}.

III. RESULTS AND DISCUSSIONS

It is proposed that the chiral superconductivity could occur in doped graphene near the van Hove singularity at $\frac{1}{4}$ hole doping⁹. Therefore, we shall first examine the possibility of superconductivity for $\frac{1}{4}$ hole doped graphene in strong electron-electron interaction limit. In this case, the band energy dispersion exhibits a quadratic saddle point at the M-points in the resulting Fermi surface when only the nearest-neighbor hopping is considered. Based on the Ginzburg-Landau theory, Nandkishore et. al argued that the chiral $d_{x^2-y^2} + id_{xy}$ combination of superconducting order that breaks the time-reversal and parity symmetry is the lowest energy in the pairing states⁵. The ground state of the $\frac{1}{4}$ -hole doped graphene with periodic strain is complicated due to the emergence of flat bands. It is reasonable that the superconducting energy gap Δ becomes position dependent and has the same period as that of the strain. This results in the emergence of the pair density wave along with the uniform chiral d-wave superconducting order, and simultaneously, the charge density wave emerging as a subsidiary order. Hence there are pair density wave order with momentum Q , the charge density wave order and the usual chiral d-wave superconductivity order in the ground state. In this paper, we adopt

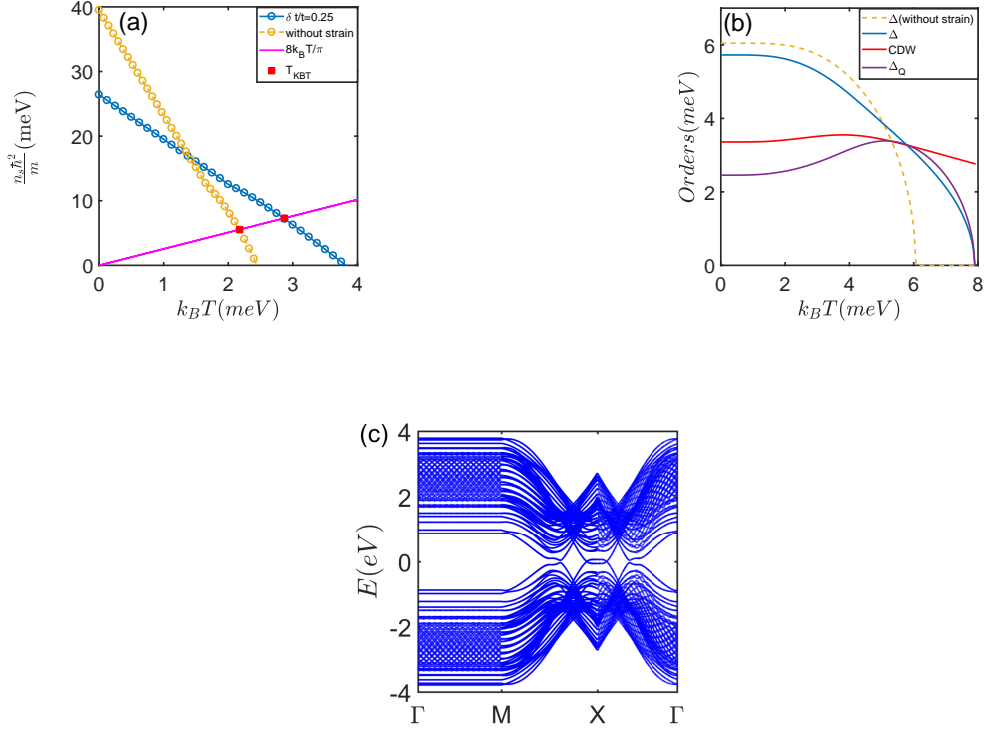


FIG. 2. (a) The superfluid weight for the $\frac{1}{4}$ -hole doped graphene with $U = 4t$ as a function of temperature without or with strain. The Berezinskii-Kosterlitz-Thouless transition temperatures are intersections of $\frac{\hbar^2 n_s(T)}{m}$ with $\frac{8k_B T}{\pi}$ as indicated by red dots. (b) The chiral d-wave superconductivity order, pair density wave order with momentum Q , and charge density wave order versus temperature for the $\frac{1}{4}$ -hole doped graphene with strain amplitude being $\frac{\delta t}{t} = 0.25$ and period being $n = 15$. The pure chiral d-wave superconductivity order in the doped graphene without strain is shown as the dash line for a comparison. (c) Quasi-particle spectrum shows that the superconducting $\frac{1}{4}$ -hole doped strained graphene is gapless.

a slightly different parameters with $n = 15$ so that the phase of pair density wave occupies larger regime. Self-consistent solved results for strained graphene with $\frac{1}{4}$ doping to the van Hove singularity are given in Fig. 2. Here the charge density wave and the pair density wave orders coexist with the chiral d-wave superconductivity order in the strained graphene are compared with the pure chiral d-wave superconductivity order in the doped graphene without strain. In Fig. 2 (b), we show the order parameters as a function of temperature. It is seen that in the presence of strain, the surviving tempera-

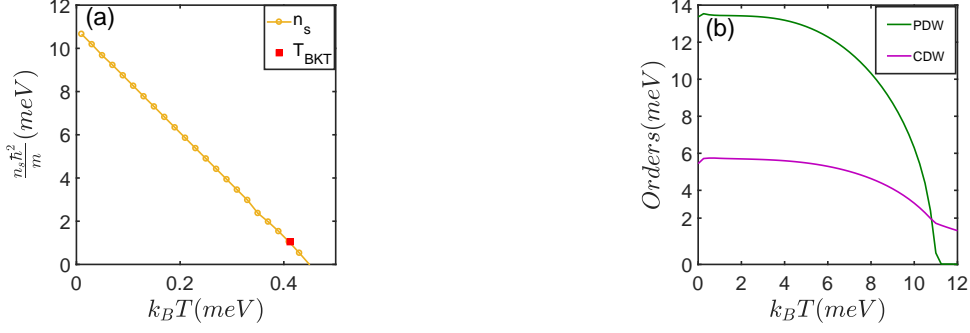


FIG. 3. (a) The superfluid weight of a pure superconducting pair-density-wave state in a lightly-doped strained graphene. Here parameters are $\delta = 0.04$, $\mathbf{U} = 4t$, $\frac{\delta t}{t} = 0.05$, and $n = 15$. The line $\frac{8k_B T}{\pi}$ is close to the temperature axis with the red dot representing the BTK transition temperature. (b) Following (a), the pair density wave order with momentum $\frac{\mathbf{Q}}{2}$ and the charge density wave order as a function of temperature.

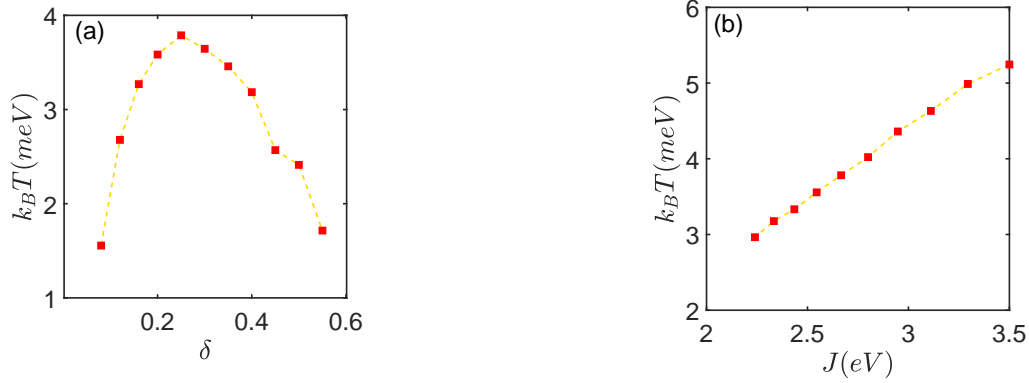


FIG. 4. (a) The BKT transition temperatures as a function of hole-doped level δ with strain amplitude being $\frac{\delta t}{t} = 0.25$ and period being $n = 15$. Here $\mathbf{U} = 4t$ and the optimal hole doping density appears near 0.25. (b) The BKT transition temperatures as a function of the strength of the spin-spin interaction with $\frac{\delta t}{t} = 0.25$ and $n = 15$. It shows an almost linear behavior, which is the same as the dependence of the transition temperature on the electron-phonon coupling when the BCS theory is specialized to a flat conduction band.

ture for superconducting orders in strained graphene is much enhanced. In the Fig. 2 (a), we show the superfluid weight as a function of temperature. It is seen that the superfluid weight decreases with the temperature linearly. This is due to that in the pair density wave state, the center of mass for each Cooper pair carries momentum so that the energy

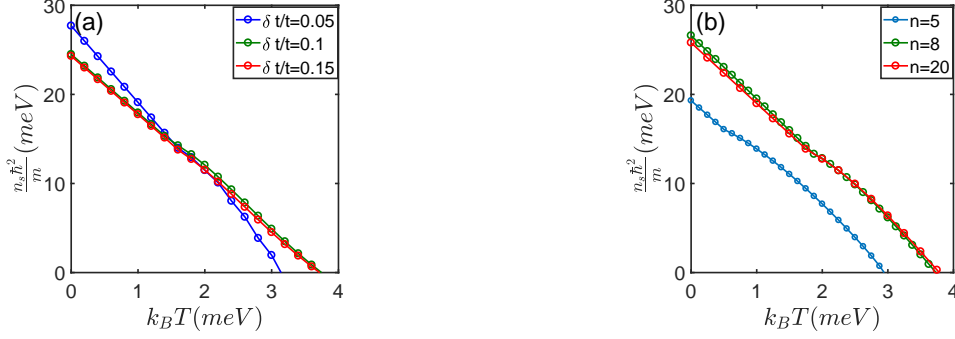


FIG. 5. The superfluid weight of the $\frac{1}{4}$ -hole doped graphene with $U = 4t$ as a function of temperature for different amplitudes of the strain with $n = 15$ (a) and periods of the strain with $\frac{\delta t}{t} = 0.25$ (b).

of the quasi-particles is Doppler shifted and becomes gapless. This is shown in Fig. 2 (c). The Berezinskii-Kosterlitz-Thouless transition temperature is determined by the intersection of $\frac{\hbar^2 n_s(T)}{m}$ with $\frac{8k_B T}{\pi}$. As indicated in Fig. 2 (a), the BKT transition temperature is lower than the temperature when the superfluid weight disappears. The enhancement of the superconducting transition temperature with strain is clearly seen: The strain enhances the BKT temperature from 25.35 K to 37.70 K about increase 50% in the $\frac{1}{4}$ -hole doped graphene.

The pair density wave with momentum Q is a trivial order induced by the periodic strain of period $L = 2\pi/Q$. It is therefore an exciting result that there is a pure superconducting pair-density-wave states (PDW) with momentum $\frac{Q}{2}$ accompanied by charge density wave along. Here there is no uniform chiral superconducting order. The PDW state has been considered as a leading candidate to characterize the pseudogap state for the high-temperature superconductivity in cuprates. In Fig. 3(a), we show how the superfluid weight of a pure PDW state changes as the temperature increases. Here the doping level is $\delta = 0.04$. Clearly, it shows the same linear behavior as that for the normal chiral d-wave superconducting state with Δ_Q being in presence. The line $\frac{8k_B T}{\pi}$ is close to the temperature axis with the red dot representing the BTK transition temperature, which is about 5 K. The thermal evolution of orders versus temperature is shown in the Fig. 3(b). The gap opening temperature is seen to be $T^* \sim 120$ K, which is much higher than the superconducting critical temperature $T_{BTK} \sim 5$ K in the lightly hole doped strained graphene. The difference between T^* and T_{BTK} is similar to the difference in

the pseudogap temperature and the superconducting transition temperature in the high-temperature cuprate superconductors and may be used to understand the origin of the pseudogap state in cuprate superconductors.

In Fig. 4(a), we show the BTK transition temperature versus the doping level δ . Clearly, in resemblance to the superconducting dome observed in high- T_c cuprate superconductors, it also exhibits a dome-like shape. We can therefore divide the superconducting region into underdoped region, the optimal doping, and overdoped region. The optimal doping level is at $\delta = \frac{1}{4}$ where the van Hove singularity occurs in the band structure of unstrained graphene. The BKT transition temperatures increase with the doping level in the underdoping region, while it decrease with the doping level in the overdoped region. The highest superconducting transition temperature is about 37.70 K in the case of $\delta = \frac{1}{4}$ with the Hubbard interaction $\mathbf{U} = 4t$. The BKT transition temperatures for different strong Hubbard interactions from $\mathbf{U} = 3t$ to $\mathbf{U} = 5t$ are shown in the Fig. 4(b). It is obvious that the BKT transition temperatures increases linearly with the residual spin-spin interaction strength $J = \frac{4t^2}{\mathbf{U}}$ even in the strong correlation limit. This is the same as the dependence of the transition temperature on the electron-phonon coupling when the BCS theory is specialized to a flat conduction band. It is a characteristics of the flat band superconductivity in contrast to the relation for the critical temperature $T_c \sim e^{-\frac{1}{\lambda}}$ in the conventional superconductors. The flat band superconductivity is thus a potential route to high-temperature superconductivity even in the presence of strong and repulsive correlation effect.

Finally, we discuss effects of the period (n) and amplitude (δt) of the strain on the superfluid weight for the $\frac{1}{4}$ hole-doped graphene with strain. As shown in the Fig. 5(a), we see that the superfluid weights for large amplitudes of strain (greater than 0.1) are almost the same near the zero temperature. As a result, the BKT transition temperature slightly increases with the creasing of the amplitude in strain beyond 0.1. Due to the periodicity imposed by the period n , the flat bands in the k space would repeat itself with the period $\frac{4\pi}{3na}$ in k_x direction. This is similar to the higher harmonics of the pair density wave Δ_{nQ} with $n = 1, 2, 3, \dots$. Furthermore, flat bands get flatter as the period of strain increases. As a result, for $n > 8$, the superfluid weights are almost the same with $n = 8$ as shown in the Fig. 5(b). However, it should be noted that as n increases, there are more flat bands, which result in higher BKT transition temperatures.

IV. CONCLUSIONS

In summary, we have shown that due to the presence of flat bands, the superconducting transition temperature for the chiral d wave superconductivity in the doped graphene with strain is enhanced approximately 50% in comparison to that of the doped graphene without strain. We also show that for the unconventional superconducting state that coexists with the charge density wave and the pair density wave in strained graphene, the superfluid weight as a function of temperature exhibits the same trend as that for pure the chiral d wave superconductivity in the unstrained graphene. The non-vanishing superfluid weight of pure pair density wave state in the lightly doped graphene demonstrates that it is a superconducting state with the critical temperature (the BTK temperature) being much lower than the gap-opening temperature. This phenomenon can be used to understand the origin of the pseudogap state observed in the high-temperature cuprate superconductors. In addition, we find that as the period and amplitude of the strain increases, the superfluid weight will saturate once flat bands emerge. Finally, we show that in resemblance to the superconducting dome observed in high- T_c cuprate superconductors¹³ and twisted bilayer graphene¹², the BKT transition temperature versus doping for strained graphene also exhibits a dome-like shape. However, unlike the exponential dependence of T_c on the spin-spin interaction strength in high- T_c cuprate superconductors, the BKT transition temperature of strained graphene depends linearly on the spin-spin interaction strength.

V. ACKNOWLEDGMENT

This work was supported by the National Science Foundation of China (Grant Nos:11804213), Scientific Research Program Funded by Shaanxi Provincial Education Department (Grant Nos:20JK0573) and Scientific Research Foundation of Shaanxi University of Technology (Grant Nos: SLGRCQD2006). C. Y. Mou was supported by the Ministry of Science and Technology (MoST), Taiwan. He was also supported by the Center for Quantum Technology within the framework of the Higher Education Sprout Project by the Ministry of

* xufenglx@snut.edu.cn

† mou@phys.nthu.edu.tw

- ¹ K. S. Novoselov, A. K. Geim, S. V. Morozov, D. Jiang, Y. Zhang, S. V. Dubonos, I. V. Grigorieva, A. A. Firsov, *Science* **306**, 666 (2004).
- ² A. H. Castro Neto, F. Guinea, N. M. R. Peres, K. S. Novoselov, and A. K. Geim, *Rev. Mod. Phys.* **81**, 109(2009).
- ³ B. Uchoa and A. H. Castro Neto, *Phys. Rev. Lett.* **98**, 146801(2007).
- ⁴ A. M Black-Schaffer and S. Doniach, *Phys. Rev. B* **75**, 134512(2007).
- ⁵ R. Nandkishore, L. S. Levitov and A. V. Chubukov., *Nature Physics* **8**, 158(2012).
- ⁶ A. M Black-Schaffer and C. Honerkamp, *J.Phys.:Comdens.Matter* **26**, 423201(2014).
- ⁷ L. Covaci and F. M. Peeters, *Phys. Rev. B* **84**, 241401(R)(2011).
- ⁸ B. Uchoa and Y. Barlas, *Phys. Rev. Lett.* **111**, 046604(2013).
- ⁹ M. L. Kiesel, C. Platt, W. Hanke, D. A. Abanin and R. Thomale, *Phys. Rev. B* **86**, 020507(R)(2012).
- ¹⁰ Y. Cao, V. Fatemi, S. Fang, K. Watanabe, T. Taniguchi, E. Kaxiras, and P. Jarillo-Herrero, *Nature* **556**, 43(2018).
- ¹¹ M. Yankowitz, S. Chen, H. Polshyn, Y. Zhang, K. Watanabe, T. Taniguchi, D. Graf, A. F. Young, and C. R. Dean, *Science* **363**, 1059(2019).
- ¹² X. Lu, P. Stepanov, W. Yang, M. Xie, M. A. Aamir, I. Das, C. Urgell, K. Watanabe, T. Taniguchi, G. Zhang, A. Bachtold, A. H. MacDonald, and D. K. Efetov, *Nature* **574**, 653(2019).
- ¹³ P. A. Lee, N. Nagaosa, X. G. Wen, *Rev. Mod. Phys.* **78**, 17(2006).
- ¹⁴ N. B. Kopnin, T. T. Heikkilä, and G. E. Volovik, *Phys. Rev. B* **83**, 220503(2011).
- ¹⁵ E. Tang and L. Fu, *Nature Physics* **10**, 964(2014).
- ¹⁶ S. Peotta and P. Törmä, *Nature communications* **6**, 8944 (2015).
- ¹⁷ A. Julku, S. Peotta, T. I. Vanhala, D. H. Kim and Törmä, *Phys. Rev. Lett.* **117**, 045303(2016).
- ¹⁸ F. Guinea, M. I. Katsnelson, and M. A. H. Vozmediano, *Phys. Rev. B* **77**, 075422(2008).
- ¹⁹ J. W. F. Venderbos and L. Fu, *Phys. Rev. B* **93**, 195126(2016).
- ²⁰ V. J. Kauppila, F. Aikebaier, and T. T. Heikkilä, *Phys. Rev. B* **93**, 214505(2016).
- ²¹ F. Xu, P. Chou, C. Chuang, T. Lee and C. Mou, *Phys. Rev. B* **98**, 205103(2018).

- ²² F. Xu and L. Zhang, *Chin. Phys. B* **11**, 117403(2019).
- ²³ V. L. Berezinskii, *Zh. Eksp. Teor. Fiz, Sov. Phys. JETP* **34**, 610(1972).
- ²⁴ J. M. Kosterlitz and D. J. Thouless, *J. Phys.C* **5**, L124(1972).
- ²⁵ J. M. Kosterlitz and D. J. Thouless, *J. Phys.C* **6**, 1181(1973).
- ²⁶ Y. Cao, S.H. Zou, X.J. Liu, S. Yi, G.L. Long, and H. Hu, *Phys. Rev. Lett.* **113**, 115302(2014).
- ²⁷ Y. Xu and C. Zhang, *Phys. Rev. Lett.* **114**, 110401(2015).
- ²⁸ B. C. Mulkerin, L. He, P. Dyke, C. J. Vale, X. Liu and H.Hu, *Phys. Rev. A* **96**, 053608(2017).
- ²⁹ X. Hu, T. Hyart, D. I. Pikulin, and E. Rossi, *Phys. Rev. Lett.* **123**, 237002(2019).
- ³⁰ A. Julku, T. J. Peltonen, L. Liang, T. T. Heikkilä and Törmä, *Phys. Rev. B* **101**, 060505(R)(2020).
- ³¹ J. E. Hirsch, *Phys. Rev. Lett.* **54**, 1317(1985).
- ³² M. Ogate and H. Fukuyama, *Rep. Prog. Phys.* **71**, 036501(2008).
- ³³ M. U. Ubbens and P. A. Lee, *Phys. Rev. B* **46**, 8434(1992).
- ³⁴ J. X. Li, C. Y. Mou, and T. K. Lee, *Phys. Rev. B* **62**, 640(2000).
- ³⁵ C. T. Shih, T. K. Lee, R. Eder, C. Y. Mou, and Y. C. Chen, *Phys. Rev. Lett.* **92**, 227002(2004).
- ³⁶ D. J. Scalapino, S. R. White and S. C. Zhang, *Phys. Rev. Lett.* **68**, 2830(1992).
- ³⁷ D. J. Scalapino, S. R. White and S. C. Zhang, *Phys. Rev. B* **47**, 7995(1993).
- ³⁸ Y. Zhong, H. Lu and H. Luo, *Eur. Phys. J. B*, **89**, 28(2016).
- ³⁹ A. I. Larkin, Y. N. Ovchinnikov. *Sov. Phys. J. Exp. Theor. Phys.*, **20**, 762(1965).
- ⁴⁰ P. Fulde, R. A. Ferrell. *Phys. Rev.* **135**, A550-63(1964).
- ⁴¹ D. F. Agterberg, J. C. Seamus Davis, S. D. Edkins. *ect. Annu. Rev. Condens. Matter. Phys.* **11**, 231-70(2020).
- ⁴² L. Salasnich, P. A. Marchetti, and F. Toigo, *Phys. Rev. A* **88**, 053612(2013).
- ⁴³ L. Liang, T. I. Vanhala, S. Peotta, T. Siro, A. Harju, P. Törmä, *Phys. Rev. B* **95**, 024515(2017).